Ono et al. *NPG Asia Materials* (2025)17:5
https://doi.org/10.1038/s41427-025-00589-5

NPG Asia Materials

ARTICLE Open Access

Direct observation of the topological pruning in silica glass network; the key for realizing extreme transparency

Madoka Ono[1,2], Yasuhito Tanabe[2], Masaya Fujioka[3], Hiroki Yamada[4], Koji Ohara[4,5], Shinji Kohara[6], Masanori Fujinami[7] and Junji Nishii[2]

Abstract

The optical transparency of silica glass significantly improves when subjected to compression at its melting temperature. Using a rare hydrostatic iso-pressure apparatus capable of reaching 0.98 GPa at 1800 °C with Ar gas as the pressure medium, we obtained centimeter-sized glass samples, allowing us to measure various properties. Both the density and refractive index increased with pressure, while the refractive index dispersion decreased monotonically. However, Rayleigh scattering intensity, and small ring structures show a minimum around 0.8 GPa. High-energy X-ray scattering analysis indicates that the short-range structure, around 4 Å, governs the monotonic trends in the averaged physical properties, such as density and refractive index. In contrast, non-monotonic changes are observed with the disappearance of intermediate-range order at around 8 Å. This simplification of structural ordering is crucial for achieving extreme transparency in silica glass. The effect of suppression of the 8 Å order is well explained by the predicted topological pruning phenomenon, where large voids and small unstable ring structures vanish, leading to the minimal light scattering under high pressure. Our experimental findings also reveal that the optimal pressure for achieving this transparency is much lower than previously predicted, which makes the process more feasible for mass-production applications.

Introduction

SiO_2 is abundant on the earth's crust, and its vitreous state, silica glass, is an indispensable material for modern society as optical fiber[1–3] and optics for lithography[4,5]. Optical fibers are undoubtedly the most important infrastructure in constructing the worldwide optical communication network. Ever since silica glass fiber was first invented in 1970, its transparency improved largely for the first ten years. However, it seems almost saturated since then, not because its specification reached a satisfactory level; the optical loss of fiber should be much lower considering the next-generation communication, quantum cryptographic, and/or quantum information are, in principle, not amplifiable[6,7]. More than 80% of the remaining optical loss is attributed to Rayleigh scattering; the scattering caused by structural fluctuations in silica glass[8]. Thus, it had long been believed that stabilizing the -Si–O- structure by thermal annealing, and/or chemical doping to accelerate the relaxation of the network is the only solution[9–11]. In 2018, M. Ono et al. proposed a new method to suppress Rayleigh scattering using pressure[12]. The scheme is based on the shrinkage of the empty spaces in silica glass, called voids that can be considered as the particles that scatter light as Rayleigh scattering[13]. The application of pressure significantly suppressed the light scattering loss. Molecular dynamics (MD) simulations predicted the further reduction of Rayleigh scattering continues until the pressure goes up to 4 GPa[14]. But it had never been examined experimentally due to the difficulty in isostatic hot compression of large-sized glass by using

Correspondence: Madoka Ono (madoka.ono.d7@tohoku.ac.jp)
[1]Graduate School of Engineering, Tohoku University, Sendai, Miyagi 980-8579, Japan
[2]Research Institute for Electronic Science, Hokkaido University, Sapporo 001-0020 Hokkaido, Japan
Full list of author information is available at the end of the article

gas media. In this study, we explored the higher-pressure region by using a hydrostatic iso-pressure apparatus capable of reaching 0.98 GPa at 1800 °C using Ar-gas media, which is one of the only two in the world[15]. We fabricated large-sized glass samples at pressures above 0.2 GPa and measured the Rayleigh scattering. Together with the investigation of the properties and the structural change using various techniques such as Raman scattering, high-energy X-ray scattering, and the refractive index with dispersion measurement, we experimentally observe the minimum Rayleigh scattering at slightly lower than 1 GPa and the structural change similar to which was predicted as topological pruning. This paper elucidates the crucial distinction between ascertaining whether the diverse physical attributes of silica glass, encompassing its optical characteristics, emanate from an averaged structure centralized on 4 Å or arise from a medium-range structural order spanning approximately 8 Å.

Materials and Methods

The original glass used for pressure application is the synthetic silica glass, AQ (product of AGC Inc, Japan) with OH concentration of approximately 50 wt. ppm, fluorine (F) and chlorine (Cl) of less than 1 wt. ppb. The fictive temperature of this original silica glass was 1330 K. For hot compression process, the glass rods of 50 mm in diameter and 70 mm in length was put into a carbon crucible in the hydrostatic isothermal pressure machine (HIP) of JUTEM CO. Ltd, Japan[15]. The pressure medium is Ar-gas. Due to the limitation of the machine, the pressure of 0.2, 0.5, 0.75, and at highest, 0.98 GPa were applied at 2073 K. After holding both the pressure and the temperature for 1 hr, the electricity was shut down and the temperature rapidly went down for 1000 K within 10 minutes, then cooled down to room temperature. The pressure was released without any further compression during cooling. The example of the pressure and temperature profiles are shown in Fig. S1. For higher pressure (from 1 to 4 GPa), a solid cubic anvil high-pressure synthesis method[16] was used to compress the silica glass at 1373 K. The sample size for the solid pressure apparatus was 4.3 mm in diameter and 5 mm in length at the largest. The surface of the compressed sample pieces was taken away to avoid a crystallized surface at the interface of the glass and the pressure medium. We prepared another silica glass samples by changing their fictive temperature, T_f, by heat treatment at 1340–1673 K being kept for 2–960 h. The details of the preparation method for these glasses are explained in[13]. T_f of the sample was determined from an infrared absorption peak at around 2260 cm^{-1} [17].

The density was measured with the Archimedean method using sample pieces larger than 10 mm in length. The refractive index and its dispersion were measured at room temperature using a refractometer (KPR-2000, Shimadzu, Kyoto, Japan) for blocks with 10 mm or 5 mm cube with six optically polished surfaces. Numerical data of the plots in Fig. 1 are listed in Table. S1. Abbe number is defined as $(n_D - 1)/(n_F - n_C)$ with the refractive index n at each wavelength of D (587.56 nm), F (486.13 nm), and C (656.27 nm), respectively. Raman spectra were measured using Raman spectroscopy (RENISHOW INVIA) under a microscope with 532 nm CW laser light. Polished plates of 1 mm thick were used. Since Raman spectroscopy is applicable to small-sized samples, we measured glass that we quenched under 1 to 4 GPa at 1373 K using

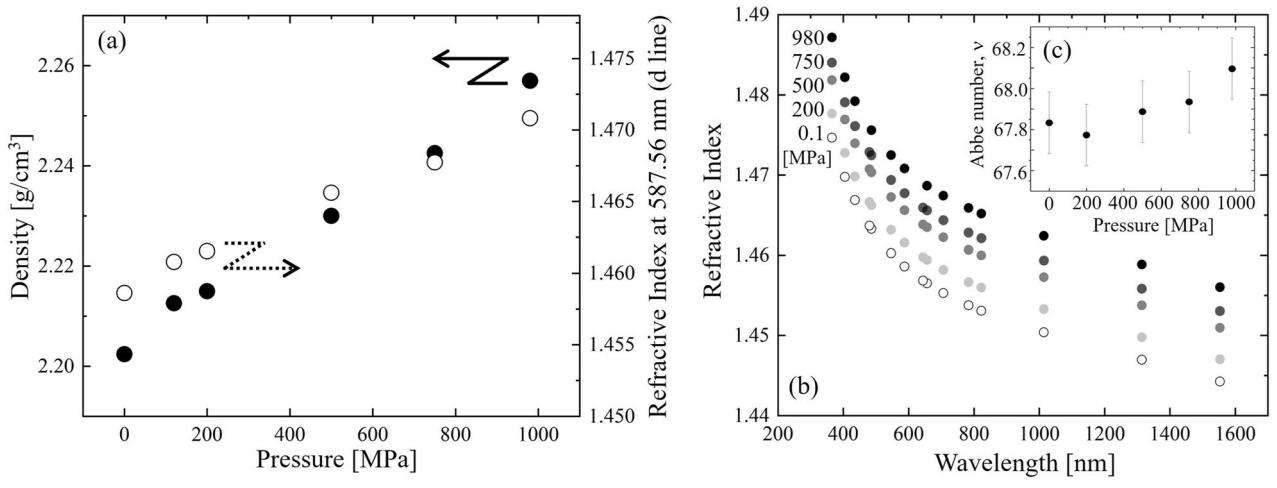

Fig. 1 Pressure dependence of density, refractive index and its dispersion. The pressure dependence of the hot compressed silica glass on (**a**) the density (black dots, plotted by the left axis) and the refractive index of silica glass (empty dots, plotted against the right axis) at *d* line (587.5 nm). **b** The dispersion of the refractive index of each sample. **c** shows the Abbe number which is defined in the context to quantify the amount of the refractive index dispersion. The higher the Abbe number, the smaller the wavelength dispersion of the sample.

cubic multianvil apparatus. The glass made under 0.2 to 0.98 GPa were by HIP at 2073 K. To examine the reproducibility and comparability, those glass made by HIP were cross-measured by the other Raman measurement system (HORIBA T64000MW/vis-NIR) with non-pressurized glass for intensity normalization. The data of 1373 K were found to be comparable with 2073 K. The details of the measurement, analysis conditions and the data connectivity are explained in Fig. S3.

Rayleigh scattering intensity measurements were conducted with 5 × 5 × 5 mm cubic sample pieces with optically polished surfaces. They were immersed in a refractive index matching liquid ($n_D = 1.4580$ at 298 K) in a cylindrical cell, to minimize stray light from the surface of the sample and the cell. The scattered light at the normal angle to the incident laser light with a wavelength of 488 nm was inserted into a 10-cm monochromator and detected with a silicon PIN detector (ET-2030, Electronics-Optics Technologies Inc.) whose signal was amplified by the current preamplifier (LI-76, NF Electronic Instruments) and put into lock-in amplifier system (EG&G Park model 5209). The light intensity of two identical pieces, which were cut out from each HIP sample were measured several times to confirm the data reproducibility. The time-average signal over 100 ms was measured as the Rayleigh scattering intensity. To obtain the absolute value of the Rayleigh scattering loss for HIP silica glasses, we compared the intensity with that of the silica glass samples with different T_f with no HIP treatment, $T_f = 1342$ and 1634 K. Further details of the Rayleigh scattering measurement can be found also in[12].

The X-ray diffraction experiments were performed in transmission geometry using beamline BL04B2 at Spring-8 with an incident energy of 61.4 keV. The incident X-ray intensity was monitored using an Ar-filled ionization chamber, and the scattered X-rays were detected by a Ge detector. A vacuum chamber was used to suppress air scattering, and the data was corrected using a standard program[18]. Each data set was normalized to give the Faber–Ziman total structure factor, $S(q)$[19].

Results and Discussions

Monotonic change of properties by compressive pressure

The density and the refractive index of the silica glass showed a monotonic increase when the applied pressure is increased. The closed and open circles in Fig. 1a correspond to the density and the refractive index, respectively. The samples were hot compressed at 2073 K. Pressure monotonically densifies the glass and induces a high refractive index. The highest densification in this region is 3%, while the refractive index increased by 1% at 0.98 GPa. The change of the density is consistent to the previously reported value of around 5% at 1 GPa (1373 K)[20]. Figure 1b shows the refractive index at various wavelengths for each sample. They are dispersion curves of the refractive index of each sample with different pressure. The detailed data of the refractive index is in Fig. S2. The cm-sized samples enabled us to obtain precise data, which systematically changes by pressure. Figure 1c shows the Abbe number ν of each refractive index dispersion curve. The value of ν linearly grows for higher pressure except for irregularity for ambient pressure of 0.1 MPa. The 0.1 MPa sample is the original silica glass which had been annealed for more than one month to obtain low T_f, while other pressure-quenched samples should have higher values due to the rapid cooling of the HIP machine. Since low T_f leads to higher ν, irregularity has occurred. The systematic increase of ν by increasing pressure, i.e. increasing refractive index, indicates that homogeneity grew with the increase of the pressure as found in ref. [21]. They made quenched glass using solid pressure medium under higher pressure of 7.7 GPa at varied temperature up to 1473 K. Our data covers a smaller region of the pressure, but within consistency to their data. In ref. [21] they concluded that the increase of ν is due to the homogeneity growth by pressure. The increase of the refractive index and ν from ambient pressure up to 0.98 GPa at 2073 K show the densification and the homogenization of the electric dipoles which govern the bandgap of silica glass (corresponding to the charge transfer transition from 2*p*-band of Oxygen to Si *d*-band) occur monotonically by pressure.

Non-monotonic change of properties by compressive pressure

On the contrary to the monotonic pressure dependence of density and the Si-O charge transfer oscillator, the structure of longer-distance, such as three-membered SiO_2 rings, showed non-monotonous trends against pressure. Figure 2a shows the Raman scattering data of the hot compressed glass. The data of the HIP-compressed samples are plotted with circles, while the ones compressed at 1373 K using multianvil cell pressure machine with solid medium of tungsten carbide (plotted with triangles) which can cover up to 4 GPa. Although the process temperature is not as high as 2073 K, they showed good connectivity at 1 GPa [S3]. The connectivity goes well with ref. [20] which indicated that temperatures higher than 1173 K lead to similar structural changes by pressure. The effective sample size of the multianvil samples with the polished vitrified surface is small (smaller than 2 mm) due to the surface crystallization from the attached pressure media. However, the Raman spectroscopy in-situ heating is possible unthe der microscope on the polished vitrified region. The insert figure in Fig. 2a shows the Raman spectra with main peak of 450 cm^{-1}, small D_1 (500 cm^{-1}) which corresponds to the number density of 4-membered rings, while D_2 (610 cm^{-1}) peak is attributable to the number density of

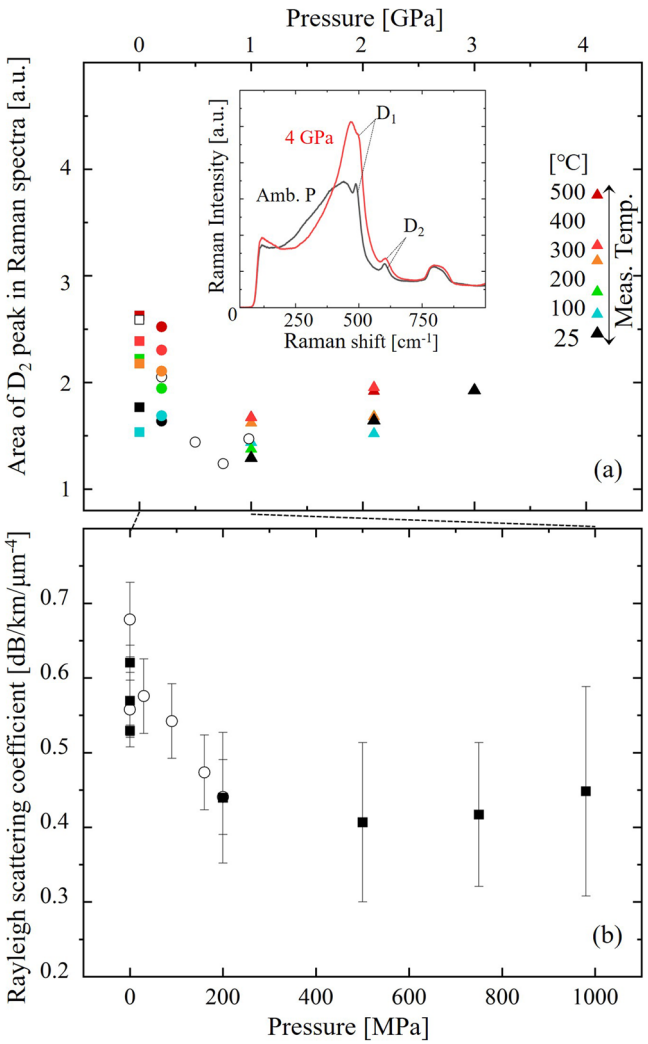

Fig. 2 Optical properties of hot compressed silica glass with non-monotonic pressure dependence. a Number density of the 3-membered ring in silica glass, estimated from the area of D_2 peak normalized by ω_3 peak height. The insert figure shows the Raman scattering spectra of the original silica glass made under ambient pressure (black) with the one quenched at 4 GPa (red). The data for $P = 1$, 2, 3, and 4 GPa are of the sample made by using solid pressure medium at 1373 K (triangles). While for $P = 0.2$ to 0.98 GPa are made by HIP at 2073 K (open and closed circles). Data for $P = 0.1$ MPa corresponds to the original glass made under ambient pressure (squares). The color of the point shows the temperature at which we measured the Raman spectra. Temperatures at which we measured in-situ are the room temperature (black), 100 °C (light blue), 200 °C (green), 300 °C (orange), 400 °C (red), 500 °C (dark red). **b** Rayleigh scattering coefficient of the silica glasses hot compressed with Ar gas media. Filled circles are new data while the open ones are taken from ref. [12]. Note that the pressure range of lower figure is up to 1 GPa, while upper axis is up to 4 GPa.

3-membered SiO_2 ring structures[22]. The increase of the small ring structures in silica glass is known as the sign of instability of the glass network structure[22,23]. Thus, the number density of 3-membered ring structures is analyzed from the area of the D_2 peak [S3]. They are plotted against pressure in Fig. 2a. The area of the D_2 peak minimized at around 1 GPa, which indicates that the 3-membered ring structure decreases by pressure up to 1 GPa from ambient pressure. Then, it increases for higher pressure from 1 GPa up to 4 GPa. The result indicates the structure becomes most stable at around 1 GPa. The color shows the temperature at which each Raman measurement is done. Open circles in Fig. 2a are the area of the D_2 peak measured at room temperature. The temperature dependence of the number density of 3-membered ring structure, which are shown by different colored dots is also the smallest at 1 GPa. The least variance at 1 GPa against temperature implies the structure becomes stable against heat at this pressure. D_1 peak intensity shows similar minimum at 1 GPa, but since D_1 peak is hardly deconvoluted from the main peak, and 4-membered ring structure is not always thought of as the representative of the unstable structure[23], we relied onto the indication of the pressure- and temperature-dependence of the D_2 peak.

Figure 2b shows the pressure dependence of the Rayleigh scattering coefficient of the HIP silica glass with pressure from ambient to 0.98 GPa. The filled dots in Fig. 2b correspond to the newly obtained data in this paper. The details of the measurement scheme can be found in ref. [12]. The open circles are taken from ref. [12], correspond to the data of samples made under pressure for a duration time of 2 hours. The previous values are consistent with the newly obtained data. It is found that the Rayleigh scattering coefficient decreases for pressure higher than 0.2 GPa, but a broad minimum exists at around 0.5–0.8 GPa. Within the data of the pressure duration time of 1 hr, the minimum Rayleigh scattering coefficient is 0.4 dB/km/μm^{-4}, which corresponds to 0.1 dB/km at 1.55 μm[12]. The minimum value is similar to those obtained for experimental conditions of 0.2 GPa for 3.5 h of pressure duration time. It is noteworthy that Rayleigh scattering rapidly decreases by pressure of about 0.2 GPa, but above that pressure, the derivative is not significantly large. From positron annihilation lifetime spectroscopy (PALS), the void size of these hot compressed glasses showed small values for 0.2 GPa and 0.98 GPa compared to that of ambient glass (initial glass before hot compression) [S4]. However, saturation of the void sizes at pressure over 0.2 GPa was also observed. The pressure dependence was not as clear as Raman and Rayleigh. The results of PALS are plotted in Fig. S4.

Overall, the trend observed by Raman and Rayleigh indicate that silica glass which is hot compressed at around 1 GPa or slightly less has stable and homogeneous intermediate range structure.

Structure and ordering change by pressure

The presence of two distinct types of pressure dependence suggests that two different structural changes occur in the silica glass network as the pressure is altered. To investigate the structural factors responsible for the pressure dependence of these properties, we performed high-energy X-ray scattering (XRS) measurements at SPring-8, using the BL04B2 beamline. The black curve in Fig. 3a shows the observed X-ray total structure factor $S(q)$ calculated from the XRS pattern of the initial silica glass with ambient pressure (0.1 MPa). The red curve in Fig. 3a is that of 0.98 GPa. As is seen, XRS patterns for q values larger than 2 Å^{-1} are almost identical. On the contrary, the $S(q)$ in the range of $q = 0$ to 2 Å^{-1} shows systematic changes with pressure, as seen in Fig. 3b, which is an expanded view of Fig. 3a. The peak called FSDP (First Sharp Diffraction Peak of q around 1.5 Å^{-1})[24,25] shifts to higher q by increasing pressure. The peak position and width of the FSDP as a function of pressure were analyzed by fitting Lorentzian curves and are shown in Fig. 3c, d, respectively. FSDP is attributed to the intermediate range ordering of the neighboring Si-O-Si chains[26,27]. Thus, the higher q shift of FSDP peak corresponds to the decrease of the intrachain distance by pressure, which is reasonable. The width of FSDP becomes smaller with increased pressure. Such sharpening of FSDP is previously reported as the indication of homogenization[20,28,29]. They reported linear change in q position and FWHM (full-width half maximum) of FSDP occurs for pressure from ambient up to 8 GPa at 1373 K and 1473 K. But in our case, we observe a small kink on their trend at 0.75 GPa, even though they are roughly linear to the pressure. This observation was made possible by the precisely controlled pressure conditions and the high accuracy of the XRS measurement technique.

Furthermore, we clearly observed the disappearance of the peak at the shoulder of FSDP (we call it SP, which is located at $q = 0.8$ Å^{-1}), by increasing pressure. The observation was successful for the first time owing to the high accuracy of the experimental techniques. Since the XRS pattern for 0.98 GPa sample seems to have only a single FSDP with no sign of an additional shoulder peak at 0.8 Å^{-1}, we subtracted the XRS patterns of 0.1 to 0.75 GPa by that of 0.98 GPa. XRS spectra with no obvious sign of SP is typical of silica glass with higher pressure[24–29]. The insert figure of Fig. 3e shows the subtracted patterns. The disappearance of SP by pressure is prominent at the lower pressure region, and gradually saturates around 0.75 to 0.98 GPa. It is indicative of the structural ordering with the scale of around 8 Å, disappears by pressure within this range. The 8 Å scale can be interpreted as the distance between atomic structures that form voids in silica glass, which have been observed to be approximately 5 to 6 Å in diameter [13, S4], with electron wavefunctions surrounding the atoms. XRS corresponds to the position of the nucleus, while positronium observes the ionic radius as the wall of the voids. Notably, the disappearance of SP and the local minimum of FWHM of FSDP occurs at a pressure slightly lower than 1 GPa (around 0.8 GPa), which coincides with the minimum of Rayleigh scattering and the number density of 3-membered rings. In Fig. 4, schematic pictures of the structure and voids in silica glass corresponding to the pressure region are drawn. From the experimental results which have a minimum at around 0.8 GPa, it is likely that the structure grows to be homogeneous by the extinction of large voids and small (3- and 4-membered) unstable rings by increasing pressure, as shown by the two left figures in Fig. 4. The trend saturates at pressure slightly lower than 1 GPa. When pressure is higher than 1 GPa, homogeneity of structures that sharpen FSDP (scale of 4 Å) continues to grow as shown by the homogeneous size of the voids in Fig. 4. But higher pressure generates 3- and 4 membered rings and their stability against heat gradually decreases. Due to the generation, densified parts should appear at a

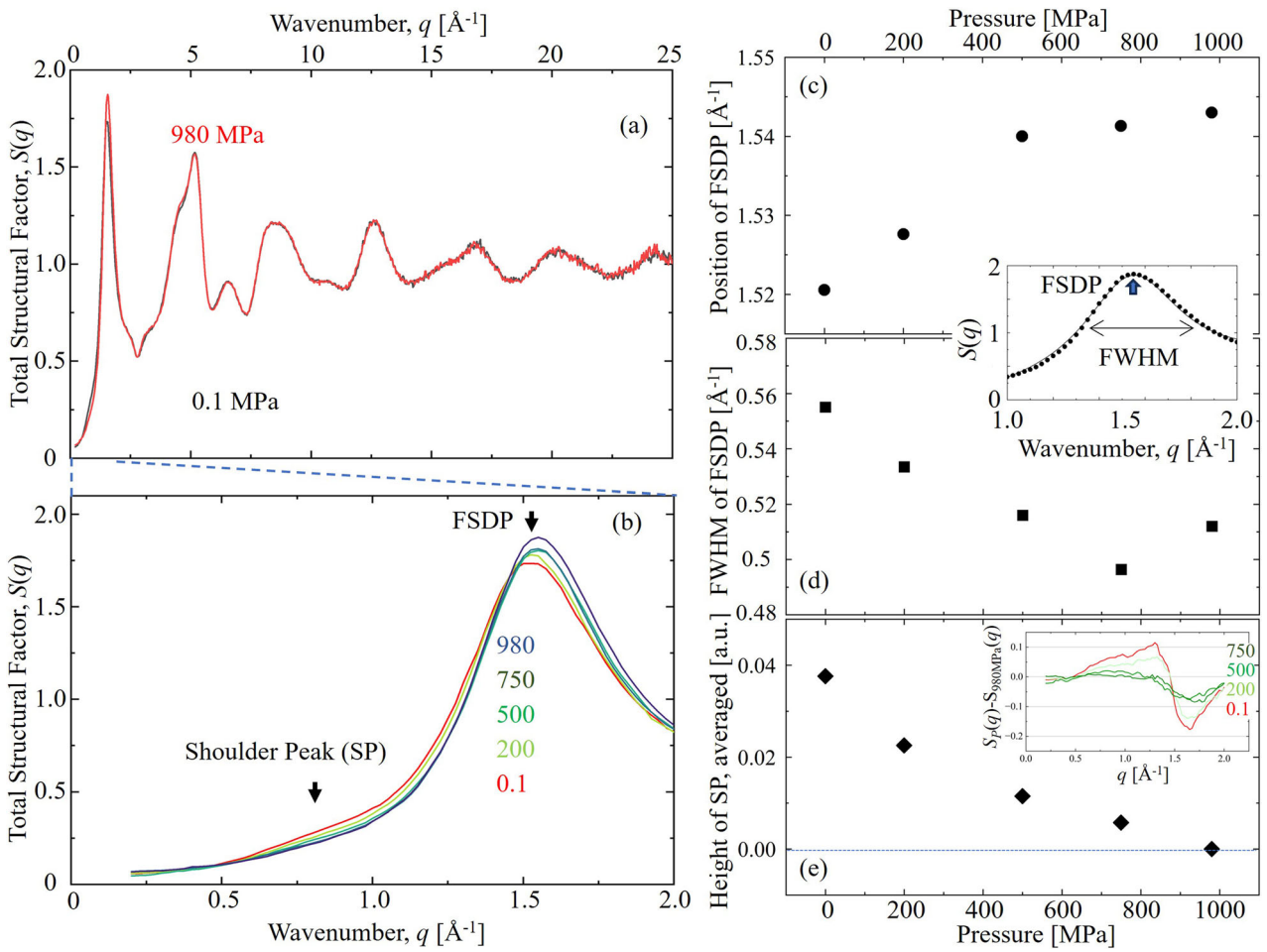

Fig. 3 The X-ray total structure factors, *S*(*q*) of of hot compressed silica glasses. a *S*(*q*) of initial glass (black) compared to the one hot compressed under 980 MPa (red). **b** *S*(*q*) of glasses hot compressed under each denoted pressure (the numbers are in MPa unit). *q* range is 0 to 2 Å^{-1}. The peak around 1.5 Å^{-1} is FSDP (First Sharp Diffraction Peak), while the one at the arrow is SP (Shoulder Peak). **c** The peak position of FSDP for each *S*(*q*) profile. **d** shows the HWHM (half width of half maximum) of the FSDP. The example of fitting FSDP with a Lorentzian curve is shown in the insert of Fig. 3d. **e** The difference of the SP peak height from that of 980 MPa. The insert figure shows Δ*S*(*q*) = (S(*q*) of each spectrum) − (*S*(*q*) of 980 MPa).

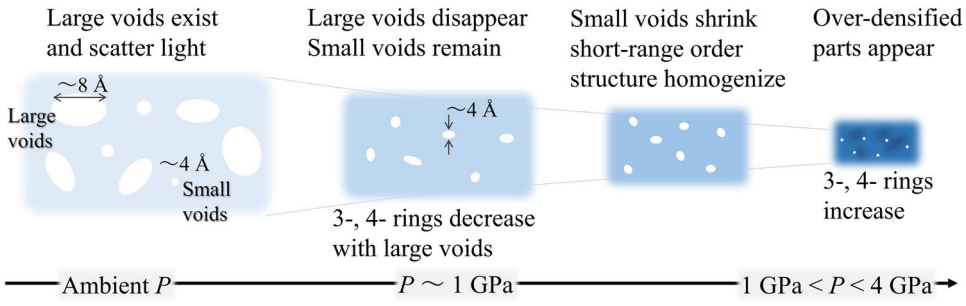

Fig. 4 Schematic pictures of the silica glass structure hot compressed under each pressure range at 2073 K. Colored parts show where the SiO_2 network occupies the space while white-painted circles show voids.

pressure higher than 1 GPa. Figure 4 indicates that density and refractive index determined by the structure part (colored part in Fig. 4) are supposed to increase continuously with higher pressure, while large voids and small rings should show different pressure dependence. Such behavior of the minimization of the number of

3-membered rings together with large voids at a peculiar pressure qualitatively matches to what is predicted as topological pruning[14]. In the simulated model, small rings appear close by large voids, and they disappear in pairs when pressure is applied. The structure is homogenized due to the reconstruction of the structures. MD predicted the silica glass network is topologically pruned to the most at the optimal pressure of 4 GPa. In this work, we observed the topological pruning phenomena experimentally. However, the pressure at which the void and 3-membered rings disappeared was 0.8 GPa and is much lower than 4 GPa. This experimental finding gives a delight future to realizing low-loss silica core glass fiber because 1 GPa is somewhat achievable pressure for industry; for example, rolling contact pressure for manufacturing steels can be 2 GPa, even though the temperature is not as high as 2000 K[30,31].

In comparison to the behavior of SP, the sharpening of FSDP, increase of density, refractive index and abbe number show no minima. They continue to change below and above 1 GPa. It is also interesting to recall the decay constant of density and refractive index under 0.2 GPa is very fast, less than 1 milli second at melting temperature, while those of void radius and Rayleigh scattering intensity were found to be longer than 1 hour[12]. Since SP corresponds to longer distance ordering (8 Å) compared to FSDP of intermediate distance ordering (4 Å), the trend of longer relaxation time for longer distance ordering is understandable. Overall, the experimental findings in this work strongly indicate the presence of two distinct types of structure order with different relaxation constants.

So far, the structures and properties of silica glass quenched under pressure of more than 1 GPa using a solid medium were investigated. With the bulk glass samples with large size obtainable by HIP, it was possible to observe the minimization of Rayleigh scattering and the growth and maximization of homogeneity at the pressure at slightly less than 1 GPa. The longer distance (8 Å) ordering seems to disappear under pressure above 1 GPa. However, the shorter distance ordering shows a continuous increase for higher pressure. This has been indicated for different temperatures as 1273 and 1373 K[20,25], the intermediate to short-range order structure which relates to optical oscillator strength is supposed to grow its homogeneity above 1 GPa and its distribution is suppressed at least up to 8 GPa. By the topological pruning, it is predicted that generation of the 5- to 6-coordination of Silicon sites instead of 4 starts to happen above 4 GPa and triggers inhomogeneity in the glass structure. Considering that 5 to 6-coordinated silicon is generated under 20 GPa at room temperature[32], but none exists up to 7.7 GPa at 1573 K[29,33], whether the coordination number of Si would increase at a pressure above 1 GPa at melting temperature should be investigated.

Summary

Through measurements of density, refractive index and its dispersion, Rayleigh scattering, Raman scattering spectra, and XRS of hot compressed silica glass, we successfully identified two distinct pressure-dependent optical properties, each arising from different structural ordering scales. The optical Rayleigh scattering is minimized at pressure around 0.8 GPa, which is coincident to the minimization of the 3-membered ring structure detected by Raman spectroscopy. They are well-explained as topological pruning phenomena, through XRS measurement which revealed the extinction of 8 Å ordering at the similar pressure. PALS does not contradict these results. The temperature dependence of 3- and 4-membered rings-structure also becomes minimum, indicating the structure becomes most stable at this pressure. Such homogeneous structure with stability was predicted to occur at 4 GPa molecular dynamics simulation as “topological pruning”, and we observed directly and experimentally the phenomena. But the experimental results have a plausible implication that the topological pruning, in reality, happens at slightly lower pressure than 1 GPa. The value is realistic for industrial application. It will be interesting to explore how shorter ordering scale continuously homogenize silica glass structure above 1 GPa. But the local homogeneity which determines Si-O oscillators, which corresponds to the width of the FSDP in XRS spectra, is independent of the long-ranged optical scattering which determines the quality and loss of silica glass fiber. Overall, this work reveals two distinct pressure-dependent phenomena in silica glass for hot compression: the local homogeneity of the long-range order structure, on the scale of about 8 Å corresponding to voids and related to Rayleigh scattering, occurs below 1 GPa; local and microscopic homogeneity increases from 1 GPa to around 4 GPa. The pressure dependence of each structural ordering scale is independent and cannot be detected solely through FSDP observations.

Acknowledgements

M. Ono thank Dr. N. Nakagawa of JUTEM CO Ltd. for his support on high-pressure HIP machines. This work is supported by Japan Society for the Promotion of Science (JSPS) for its support through KAKENHI Grant Nos. 20H05880, 21H01835, 21K19016, and 24K01371. The high-energy X-ray total scattering experiments at SPring-8 were approved by the Japan Synchrotron Radiation Research Institute under proposal nos. 2020A1698, 2021A1189, and 2022A1261.

Author details

[1]Graduate School of Engineering, Tohoku University, Sendai, Miyagi 980-8579, Japan. [2]Research Institute for Electronic Science, Hokkaido University, Sapporo 001-0020 Hokkaido, Japan. [3]National Institute of Advanced Industrial Science and Technology (AIST), Aichi 463-8560, Japan. [4]Japan Synchrotron Radiation Research Institute (JASRI), Kouto, Hyogo 679-5198, Japan. [5]Faculty of Materials for Energy, Shimane University, Matsue, Shimane 690-8504, Japan. [6]National Institute for Materials Science (NIMS), Tsukuba, Ibaraki 305-0047, Japan. [7]Department of Applied Chemistry & Biotechnology, Chiba University, Inage, Chiba 263-8522, Japan

Author contributions
M.O. designed the study, took primary responsibility for writing and revising the manuscript. Y. T. contributed to the preparation of samples, measurement, and analyses. M. F. supervised multianvil cell pressure machine tests, while H. Y. and K. O. supported experiments at Spring-8. S. K. performed the X-ray scattering spectroscopy and its analysis. M. F. conducted and analyzed the positron annihilation lifetime spectroscopy. J. N. revised the manuscript. All authors discussed the results and commented on the manuscript.

Data availability
Data is available upon request to the corresponding author, M. O.

Conflict of interest
We declare there is no conflict of financial interests in relation to the work described here.

Ethics approval and consent to participate
This paper is not applicable as it does not report on or involve any animals, humans, human data, human tissue or plants.

Publisher's note
Springer Nature remains neutral with regard to jurisdictional claims in published maps and institutional affiliations.

Supplementary information The online version contains supplementary material available at https://doi.org/10.1038/s41427-025-00589-5.

Received: 22 October 2024 Revised: 20 December 2024 Accepted: 21 January 2025
Published online: 21 February 2025

References

1. Crisp, J. & Elliott, B. *Introduction to Fiber Optics*. Third Edition Elsevier Ltd. (2005).
2. Kanamori, H. Fifty Year History of Optical Fibers. *SEI TECHNICAL REVIEW* **91**, 15–22 (2020).
3. Kanamori, H. Transmission of loss of Optical fibers; Achievements in half century. *IEICE Trans. Commun.* **E104–B**, 922–933 (2021).
4. Ikuta, Y. et al. New silica glass (AQF) for 157-nm lithography. *Optical Microlithography XIII*, (5 July 2000); https://doi.org/10.1117/12.388990.
5. Toombs, J. T. 3D PRINTING Volumetric additive manufacturing of silica glass with microscale computed axial lithography. *Taylor Sci.* **376**, 308–312 (2022).
6. Dieks, D. Communication by EPR devices. *Phys. Lett. A* **92**, 271–272 (1982).
7. Azuma, K. et al. Quantum repeaters: From quantum networks to the quantum internet. *Rev. Mod. Phys.* **95**, 045006 (2023).
8. Agrawal, G. P. Optical Communication: Its History and Recent Progress. In: Al-Amri, M., El-Gomati, M., Zubairy, M. (eds) Optics in Our Time. *Springer*, (2016).
9. Saito, K. et al. Limit of the Rayleigh Scattering loss in silica fiber. *Appl. Phys. Lett.* **83**, 5175 (2003).
10. Saito, K., Kakiuchida, H. & Ikushima, A. J. Light-scattering study of the glass transition in silica, with practical implications. *J. Appl. Phys.* **84**, 3107–3112 (1998).
11. Saito, K., Kakiuchida, H. & Ikushima, A. J. Fictive temperature dependence of the density fluctuations. *J. Appl. Phys.* **94**, 4824–4827 (2003).
12. Ono, M., Aoyama, S., Fujinami, M. & Ito, S. Significant suppression of Rayleigh scattering loss in silica glass formed by the compression of its melted phase. *Opt. express* **26**, 7942–7948 (2018).
13. Ono, M., Hara, K., Fujinami, M. & Ito, S. Void structure in silica glass with different fictive temperatures observed with positron annihilation lifetime spectroscopy. *Appl. Phys. Lett.* **101**, 164103 (2012).
14. Yang, Y., Homma, O., Urata, S., Ono, M. & Mauro, J. C. Topological pruning enables ultra-low Rayleigh scattering in pressure-quenched silica glass. *npj Comput. Mater.* **6**, 139 (2020).
15. JUTEM CO Ltd., Yamaguchi, Japan; https://www.jutem.co.jp/.
16. Fujioka, M. et al. High-Pressure Diffusion Control: Na Extraction from $NaAlB_{14}$. *Chem. Mater.* **35**, 3008–3014 (2023).
17. Agarwal, A., Davis, K. M. & Tomozawa, M. A simple IR spectroscopic method for determining fictive temperature of silica glasses. *J. Non-Cryst. Solids* **185**, 191–198 (1995).
18. Ohara, K., Onodera, Y., Murakami, M. & Kohara, S. Structure of disordered materials under ambient to extreme conditions revealed by synchrotron x-ray diffraction techniques at SPring-8—recent instrumentation and synergic collaboration with modelling and topological analyses. *J. Phys.: Condens. Matter* **33**, 383001 (2021).
19. Faber, T. E. & Ziman, J. M. A theory of the electrical properties of liquid metals III. the resistivity of binary alloys. *Philos. Mag.: A J. Theor. Exp. Appl. Phys.* **11**, 153–173 (1964).
20. Guerette, M. et al. Structure and Properties of Silica Glass Densified in Cold Compression and Hot Compression. *Sci. Rep.* **5**, 15343 (2018).
21. Masuno, A. et al. Higher refractive index and lower wavelength dispersion of SiO_2 glass by structural ordering evolution via densification at a higher temperature. *RSC Adv.* **6**, 19144–19149 (2016).
22. Geissberger, A. E. & Galeener, F. L. Raman studies of vitreous SiO_2 versus fictive temperature. *Phys. Rev. B* **28**, 3266–3271 (1983).
23. Uchino, T., Kitagawa, Y. & Yoko, T. Structure, energies, and vibrational properties of silica rings in SiO2 glass. *Phys. Rev. B* **61**, 234–240 (2000).
24. Susman, S. et al. Intermediate-range order in permanently densified vitreous SiO_2: A neutron-diffraction and molecular-dynamics study. *Phys. Rev. B* **43**, 1194 (1991).
25. Inamura, Y., Katayama, Y., Utsumi, W. & Funakoshi, K. Transformations in the Intermediate-Range Structure of SiO_2 Glass under High Pressure and Temperature. *Phys. Rev. Lett.* **93**, 015501 (2004).
26. Mei, Q., Benmore, C. J. & Weber, J. K. R. Structure of Liquid SiO_2: A Measurement by High-Energy X-Ray Diffraction. *Phys. Rev. Lett.* **98**, 057802 (2007).
27. Hirata, A. et al. Direct observation of the atomic density fluctuation originating from the first sharp diffraction peak in SiO_2 glass. *NPG Asia Mater.* **16**, 25 (2024).
28. Onodera, Y. et al. Understanding diffraction patterns of glassy, liquid and amorphous materials via persistent homology analyses. *J. Ceram. Soc. J.* **127**, 853–863 (2019).
29. Onodera, Y. et al. Structure and properties of densified silica glass: characterizing the order within disorder. *NPG Asia Mater.* **12**, 85 (2020).
30. Uppaluri, R. & Helm, D. Thermomechanical characterization of 22MnB5 steels with special emphasis on stress relaxation and creep behavior. *Mater. Sci. Eng.: A* **658**, 301–308 (2016).
31. Okayasu, M. & Yang, L. Influence of microstructure on the mechanical properties and hydrogen embrittlement characteristics of 1800 MPa grade hot-stamped $^{22}MnB_5$ steel. *J. Mat. Sci.* **54**, 5061–5073 (2019).
32. Sato, T. & Funamori, N. High-pressure structural transformation of SiO_2 glass up to 100 GPa. *Phys. Rev. B* **82**, 184102 (2010).
33. Sato, S. et al. Synthesis of hyperordered permanently densified silica glasses by hot compression above the glass transition temperature. *J. Ceram. Soc. Jpn.* **132**, 427–433 (2024).